ISTANBUL UNIVERSITY PRESS

Comparative assessment of different nanobodies that inhibit the interaction of B7-1/2 with CD28 as a potential therapeutic target for immune-related diseases by molecular modeling

Halil Ibrahim Bulut[1] ⓘ, Nail Besli[2] ⓘ, Guven Yenmis[3] ⓘ

[1]Istanbul University-Cerrahpasa, Faculty of Medicine, Medical Program, Istanbul, Turkiye
[2]Health Sciences University, Faculty of Medicine, Department of Medical Biology, Istanbul, Turkiye
[3]Biruni University, Faculty of Medicine, Department of Medical Biology, Istanbul, Turkiye

ORCID IDs of the authors: H.İ.B. 0000-0002-9076-8296; N.B. 0000-0002-6174-915X; G.Y. 0000-0002-6688-9725

ABSTRACT

Background and Aims: Active T cells are central players in the self-defense system as well as in immune-related diseases. Being crucial for T cell activation, the interaction of B7-1/2 with CD28 is associated with T cell activation-related diseases such as alloreactivity in transplantation and autoreactivity in autoimmune disorders. Nanobodies are the recombinant variable and single-domain smallest antigen-binding fragments. The focus of this study is to investigate the interactions between B7-1/2 and eight antibodies at the molecular level utilizing computational methods, and to guide the best nanobody for in-vitro and in-vivo studies about immunosuppressive

Methods: After receiving the 3D models of agents via Robetta, molecular docking techniques were used to compare the binding modes and affinities of six nanobodies and two FDA-approved fusion protein models against B7-1/2 (CD80/CD86).

Results: According to our *in silico* outputs, we selected the top of model clusters from HADDOCK 2.4 (Z-Score of CD80/CD86:-2.7 to -1.3/-2.1 to -2.1) and distinguished that 1A1 and 1B2 have higher affinities than Belatacept and Abatacept for the percentage of a calculation scale.

Conclusion: Our findings suggest that selected nanobodies show higher affinity by interacting with the CD80/86 epitope regions and provide helpful insights into the design and improvement of further computational investigations of nanobody modeling.

Keywords: Immunosuppression, Immune-related diseases, Nanobody, B7 Antigens, Molecular modeling

INTRODUCTION

Activated T cells are significant players in immune responses. The activation of T cells is dependent on antigen provided by APCs (antigen-presenting cells) through the MHC (major histocompatibility complex)-TCR (T cell receptor) interaction, which is the first signal and antigen-specific pathway required for T-cell activation. However, the MHC-TCR interaction is hardly sufficient for T-cell activation owing to the low affinity of the TCR for the specific MHC-peptide complex, so there is a second signaling pathway that requires T-cell activation (Abbas et al., 2019). The second pathway stabilizes the weak MHC-TCR interaction with stronger non-specific protein interactions and leads to an increase in the antigen presentation capacity and T cell activation ability of

289

APCs (Janeway Jr et al., 2001). The B7-1/2(CD80/CD86)-CD28 is one of the most prominent second signaling interactions. The interaction component is CD28, which is expressed on all naïve T cells, interacting with the proteins B7-1(CD80) and B7-2(CD86) as the co-stimulatory signal or interacting with CTLA4 as the inhibitory signal (Goronzy & Weyand, 2008). In this regard, Green et al. highlighted the significance of B7-1/,2-CD28 and its interaction associated with the deficient germinal center formation and impaired cytotoxic lymphocyte functions in CD28-deficient mice (Green et al., 1994). In conclusion, these features of the B7-1/2-CD28 interaction are compulsory for T-cell-mediated immune responses.

The role of autoreactive T lymphocytes in autoimmune diseases is pivotal. T cell mediated-autoreactivity responses, which are significant signals of B7-1/2-CD28, commence with the presentation of the body's own antigens to T cells (Khan & Ghazanfar, 2018). Abatacept, a CTLA-4 recombinant fusion protein, is a well-reported agent in experimental autoimmunity such as systemic lupus erythematosus (Crepeau & Ford, 2017). Also, Abatacept is the first FDA-approved drug with the ability to block the B7-1/2-CD28 pathway and is prescribed for distinct autoimmune diseases such as psoriasis and rheumatoid arthritis (Ansari et al., 2017).

Alloreactive T lymphocytes mediate acute graft rejection. Alloreactivation of T cells is contingent on antigen presentation. The B7-1/2-CD28 pathway is a positive stimulator of antigen presentation and also enhances T cell alloreactivity, therefore, inhibiting that pathway has gained importance. In previous studies, Abatacept was tested to block B7-1/,2-CD28 in non-human kidney transplant models (Larsen et al., 2005). However, Abatacept failed to prolong graft survival due to the insufficient blockade of B7-1 and B7-2 proteins (Ansari et al., 2017). Subsequently, Belatacept, a higher avidity and selectivity fusion protein than Abatacept as binding to B7-1 and B7-2, was developed (Larsen et al., 2005). Like Abatacept, Belatacept is FDA-approved for the prevention of acute kidney transplant rejection. It has been reported that Belatacept is a safer agent due to both its non-nephrotoxic and nephroprotective properties compared to other immunosuppressive agents (Noble et al., 2019).

Nanobodies (NBs), recombinant variable domains of heavy chain-only antibodies, are in the range of 12–14 kDa molecular weights (Jovčevska & Muyldermans, 2020). Due to their small size, NBs exhibit better tissue penetration than conventional monoclonal antibodies with the features of unique solubility, high stability, ease of production, and quick clearance from the blood (Sun et al., 2021). These properties are regarded as very promising and NBs could become potential therapeutic agent candidates for autoimmune disorders such as against TNF and IL-6 in rheumatoid arthritis and, IL-17 in Psoriasis in phase-1 and phase-2 clinical trials (Jovčevska & Muyldermans, 2020).

Several scientific papers and patents containing information on therapeutic agents indicate that various agents, such as fusion proteins and NBs, are designed to target the B7-1/2-CD28 interaction. These include the FDA-approved fusion protein Belatacept for kidney transplants and the FDA-approved fu-

sion protein Abatacept for rheumatoid arthritis. These therapeutic agents, which can be designed with various engineering technologies, might have a different ability to bind B7-1 and B7-2 proteins, even in terms of variations in amino acid sequences. For instance, even though the amino acid sequence of Belatacept differs from Abatacept by only two amino acids, there is a significant affinity difference between them (Larsen et al., 2005). Therefore, there is a demand to assess the most effective candidates among various therapeutic agents.

In silico analysis of agent-target, protein interactions play a substantial role in augmenting the yield of drug research and facilitating the development of new therapies before experimental and clinical approvals (Song et al., 2013).

In the current study, the molecular docking process was conducted under the inspiration of experimental and clinical findings. This study is the first attempt to show the interaction of B7-1 and B7-2 with eight agents by analyzing docking poses. Moreover, it would also be highly advantageous to assess various immunosuppressive nanobodies before preclinical pharmacokinetic investigations. The main aim of this study is to recommend the best nanobody for *in vitro* and *in vivo* studies about immunosuppressive therapy by comparing the binding affinity of eight agents to B7-1 and B7-2. This is a comprehensive study that uses the predicted structure of agent models to simulate interaction with target antigens throughout molecular modeling.

MATERIALS AND METHODS

Pre-preparation for docking procedure obtaining the 3D structure of protein and peptide

First, the crystal structure of human T-lymphocyte activation antigen CD80(PDB ID:1DR9)/ CD86(PDB ID:1I85) in PDB format was downloaded from PDB (Protein Data Bank) at http://www.rcsb.org/. All NBs, Belatacept, and Abatacept sequence information including Complementarity-determining regions (CDRs) were obtained from https://patentscope.wipo.int (see supplement file 1). Then, each of the amino acid sequences was subjected to the Robetta (Raman et al., 2009; Song et al., 2013). In this process, RoseTTAFold was used. All settings were left as default and generated five 3D-structure models having selected the most accurate with comparative assessment according to the confidence score that indicates the accuracy of model protein in terms of predicted GDT (1.0 good, 0.0 bad). RoseTTAFold is a method that is based on the principle of simultaneously considering patterns in protein sequences which show how a protein's amino acids interact with each other. The method also shows the possible three-dimensional structure of a protein. In this construction, primer, 2D, and 3D information flow back and forth, permitting the network to collectively sense the connection between chemical parts of a protein and its folded structure. The epitope information of CD80/CD86 was fetched from Immune Epitope Database (Vita et al., 2012).

Energy minimization and assessment of model protein structures

The energy minimization of 3D model protein structures was subjected to the minimization method in chimera 1.14 (Pet-

tersen et al., 2004). The default was the steepest descent:100 with 0.02 step sizes, without fixing any atoms, followed by 10 steps of conjugate gradient steps with 0.02 step size (Å) minimization. To control the quality of the model peptides, we evaluated the analysis of structural quality using Qualitative Model Energy Analysis (QMEANDisCo) (A. Waterhouse et al., 2018). In addition, Ramachandran plots were drawn to assign key secondary structures to specific regions in the plot.

Visualization of molecular modeling simulations using Jalview and PyMOL

The primary structure of CD80/CD86 was colored to exhibit the epitope regions by the Jalviewprogram (A. M. Waterhouse et al., 2009), which is an application designed for the sort of deep sequence analysis required when investigating novel protein or RNA sequence families to figure out how their sequences associate with structure and function (see supplement files). The PyMOL (Schrödinger, LLC, 2015) software is a molecular visualization system, utilized to illustrate the tertiary structure of antigen-NBs and to analyze the molecular modeling results at an atomic level. All complexes of protein-peptides modeling were obtained via the HADDOCK 2.4 web server which is an integrative platform for the docking of biomolecular complexes. It was adjusted to the default settings and provided active residues (epitope regions on CD80/CD86 and CDRs on nanobodies) for docking on both molecules.

RESULTS

The understanding of the 3D structures of target proteins is critically essential for plausible protein engineering. Until recently, there has been some convincing evidence that the role of CD80/CD86 in blocking interaction with CD28 as a treatment for Immune-Associated Diseases (Crepeau & Ford, 2017; Khan & Ghazanfar, 2018). Although Belatacept and Abatacept are the fusion proteins currently used for this therapy, some peptide agents such as NBs might also promise targets as potential therapeutic agents thanks to their more efficient properties (Jovčevska & Muyldermans, 2020).

In Table 1, the confidence scores of 3D models of agents are given and they display the accuracy of models in terms of predicted GDT scores (with 1.0 being good, 0.0 being bad). Besides, we evaluated the model peptides in the analysis of quality estimate as well as the outputs of Ramachandran plots using the QMEAN assessment tool (A. Waterhouse et al., 2018). Accordingly, all predicted model proteins are of a quality to be subjected to the docking procedure. All CDR positions of the listed antibodies in Table 1 with their sequences are available, as well as target regions of proteins and peptides for the molecular docking in supplement file 1.

Docking outputs of CD80/CD86 with each of the nanobody models and fusion proteins

This study attempts to investigate the binding mode and affinity between CD80/CD86 epitopes and CDRs of six model NBs compared to Abatacept and Belatacept peptides that block the interaction of CD80/CD87 and CD28 proteins by the analysis of polar contacts between the peptide chains. Herein, we performed molecular modeling to design the appropriate
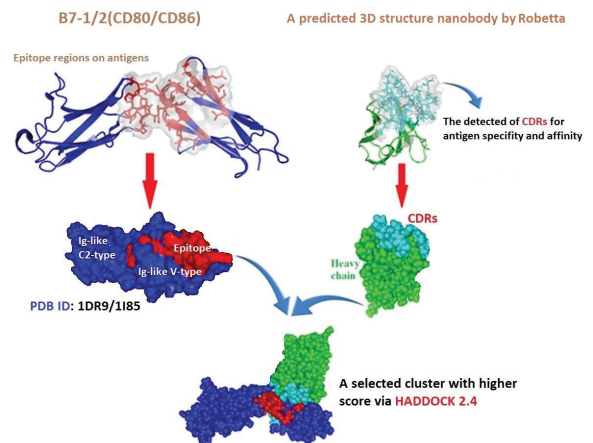
Figure 1. The description of the molecular modeling of B7-1/2 and model nanobodies.

Table 1. The table presents the epitope region (107-131aa) of CD80 interactingwith the residuesof the CDRs of the model NBs and reference peptides and Robetta confidence scores in the structural assessment of models. Polar contact residues in the CDRs are indicated in red font.

	Robetta confidence score	Length(aa)	Fetched CDR positions		
			CDR$_1$	CDR$_2$	CDR$_3$
Belatacept	0.68	357	-	-	-
Abatacept	0.66	357	-	-	-
CD8086PMP1A1	0.86	125	IDAMG	SIGRSGNSATNVDSVKG	ATRRAYLPIRIRDYIY
CD8086PMP1E11	0.86	124	YSAIG	YISSSDGSTYYADSVEG	GGPFTVSTMPWLANY
CD8086PMP2B4	0.88	120	IYTMG	AITSGGSTNYADSVKG	IAHEEGVYRWDE
CD8086PMP2B10	0.94	118	DNTMN	SLSIFGATGYADSVKG	GPVRRSR LEY
CD8086PMP1B2	0.89	123	SYVMG	AIIGRDIGTYYADSVKG	DSRSRLSGIRSAYDY
CD8086PMP1C7	0.87	123	DYAAG	AINWSGGSTYYADSVKG	GWGRTTVLADTVVY

Table 2. The table indicates the epitope region (59-74aa) of CD86 interacting with the residues of the CDRs of the model NBs and reference peptides and Robetta confidence scores in the structural assessment of models. Polar contact residues in the CDRs are indicated in red font.

	Robetta confidence score	Length(aa)	Fetched CDR positions		
			CDR$_1$	CDR$_2$	CDR$_3$
Belatacept	0.77	357	-	-	-
Abtacept	0.75	357	-	-	-
CD8086PMP1A1	0.86	125	IDAMG	SIGRSGNSATNVDS-VKG	ATRRAYLPIRIRDYIY
CD8086PMP1E11	0.86	124	YSAIG	YISSSDGSTYYADSVEG	GGPFTVSTMPWLANY
CD8086PMP2B4	0.88	120	IYTMG	AITSGGSTNYADSVKG	IAHEEGVYRWDE
CD8086PMP2B10	0.94	118	DNTMN	SLSIFGATGYADSVKG	GPVRRSRLEY
CD8086PMP1B2	0.89	123	SYVMG	AIIGRDIGTYYADSVKG	DSRSRLSGIRSAYDY
CD8086PMP1C7	0.87	123	DYAAG	AINWSGGSTYYADS-VKG	GWGRTTVLADTVVY

Table 3. The table presents the statistics of top clusters from molecular docking results. The top clusters are the most reliable according to HADDOCK 2.4. The Z-score of each cluster designates how many standard deviations from the mean these clusters are placed in terms of score (lower is better). The polar contacts formed in the docking complex are between the residues from the epitope of CD80 and CDRs of NBs. In the write-up of the residues, the first one is in the epitopes and the next one is in the CDRs and each contact between residues is separated by "/".

Model Antibody	HADDOCK score	Target Domain(Ig-like V-type) of CD80(107-131)	RMSD from the overall lowest-energy structure	Z-Score	Residues from Epitope of CD80 and CDRs of NBs	Contact Distance (Å)
1A1	-82.6 +/- 7.7	RPSDE-GTYECVVLK YEKDAFKREHL	1.4 +/- 0.9	-2.7	Y121-Y104,L105/K123-L105/D124-R53,S54,S57	2.3-2.5/2.1/1.7-2.3
2B4	-88.4 +/- 3.6	RPSDE-GTYECVVLK YEKDAFKREHL	0.7 +/- 0.5	-2.2	K120-S53/E122-H100/D124-Y105,G103/Y121-S56/K120,K127-N58/R128-D61/E129-K65	2.0-2.4/1.9-2.5/1.7-2.6/1.5-1.6/1.8-2.0
1C7	-73.5 +/- 2.6	RPSDE-GTYECVVLK YEKDAFKREHL	14.0 +/- 0.1	-2.2	E122,K123-K65/R128-V105	1.7-2.6/2.0
1E11	-71.4 +/-5.6	RPSDE-GTYECVVLK YEKDAFKREHL	0.5 +/- 0.3	-1.8	D124-S105/K127-S54/R128-N112,L110/Q67,K70-Y113	1.8/1.6/1.8-2.5/1.7-2.6
2B10	-85.9 +/- 8.9	RPSDE-GTYECVVLK YEKDAFKREHL	0.8 +/- 0.5	-1.8	E122-R102/R128-R104,R102/ E115-R102	1.8-2.3/1.8-2.1/1.7-2.2
1B2	-83.4 +/- 5.3	RPSDE-GTYECVVLK YEKDAFKREHL	1.4 +/- 1.0	-1.8	K70-D55/R128-D55,R54/R63,Y65-Y59/Y121,K123-R108/ D124-R101,R103	1.6/1.7-2.5/1.9-2.4/1.9-2.0/1.6-1.7
Belatacept	5.0 +/- 14.7	RPSDE-GTYECVVLK YEKDAFKREHL	1.4 +/- 1.0	-2.0	E111,T113-H2/ R128-Y90 / L131-A7 / E133-K93 / R63-D41/Y65- A40,S42	1.6-1.9-2.8/1.6-2.4/1.9/1.7-1.8
Abatacept	20.1 +/- 7.0	RPSDE-GTYECVVLK YEKDAFKREHL	15.4 +/- 0.6	-1.3	Y121-A7/ D124-V8,L10/ R128-Q80	2.3/1.7,1.9/2.3-2.2

Table 4. The table provides that polar contacts formed in the docking complex are between which residues from the epitope of CD86 and CDRs of nanobodies.

Model Antibody	HADDOCK score	Target Domain (Ig-like V-type) of CD86 (59-76)	RMSD from the overall lowest-energy structure	Z-Score	Residues from Epitope of CD147 and Antibody CDRs	Contact Distance (Å)
1B2	-85.2 +/- 3.2	DQ ENLV-LNEVYLG-KEKFD	0.3 +/- 0.2	-2.1	K72-E46,F47,S63/D76-Y60	2.3/1.5-2.4
1A1	-118.4 +/- 0.9	DQ ENLV-LNEVYLG-KEKFD	0.6 +/- 0.4	-2.0	K74-A58/D76-S54,G55,N56,S57/F75-S57	1.7/1.8-2.6/1.7-2.5
2B10	-83.7 +/- 4.7	DQ ENLV-LNEVYLG-KEKFD	5.7 +/- 0.2	-1.9	K74-T57/D76-S53,R101	2.2/1.7-1.8
1E11	-87.4 +/- 3.7	DQ ENLV-LNEVYLG-KEKFD	10.3 +/- 0.2	-1.5	H79-E65 /K74,S77-Y59/ M120-Y31,S53/H113-S54	1.7/2.1-2.2/2.2-2.4
1C7	-83.8 +/- 2.4	DQ ENLV-LNEVYLG-KEKFD	0.7 +/- 0.4	-1.4	N62-T109 / Y69-Y60/D76-S57,T58/S77-R102	1.7-2.4/2.5/2.1/1.9
2B4	-85.0 +/- 6.5	DQ ENLV-LNEVYLG-KEKFD	6.7 +/- 0.2	-1.1	D76-T52,G55,S56/Y69-T57,K64/S78-H100	1.7-2.6/1.8-2.4/2.6
Belatacept	-32.0 +/- 2.4	DQ ENLV-LNEVYLG-KEKFD	1.2 +/- 1.2	-1.8	Q60,N62-Q43/H79-T45/ Y69-L58/K72-Y52	2.8-2.4/2.3/2.3/2.0
Abatacept	-18.7 +/- 6.7	DQ ENLV-LNEVYLG-KEKFD	13.7 +/- 0.3	-1.5	Q60-S70/E61-S70,S71/ N62-E57/E67-T67/K72-R14,G15,Q80/E73-Q80	2.0/2.3,1.9/2.1/2.1

tertiary structure of the six patented nanobody models and opted for both Belatacept and Abatacept, which are FDA-approved drugs, as reference peptides.

The docking scores and the residues of polar contacts between CD80/CD86 and peptide models are listed in Tables 3 and 4. As can be seen from Tables 3 and 4, residues formed polar bonds with CDRs of peptide models from the epitopes of CD80 and CD86 are mentioned. Considering Belatacept and Abatacept as the variants of CTLA-4, the Ig-like V-type domain, where CTLA4 interacts with CD80/86, was identified as the active binding site for the molecular docking. Although CDR1,2,3 of nanobody models are actively processed for molecular docking in Tables 1 and 2, no polar bond formation was observed in the CDR1 region.

The docking scores between target CD80/CD87 and NBs are listed in Tables 3 and 4. Based on the Z-score value, the best clusters among all cluster results of CD80/CD87 and nanobody models were selected. In this respect, during submitting to the HADDOCK web server, since the obtained epitopes and CDR regions were prioritized as active residues (directly involved in the interaction), docking results might be more dependable. Overall, all clusters might achieve good outcomes, even if the predicted peptide model structures when an uncertain epitope region and variable CDRs are revealed.

DISCUSSION

All docking processes are linked to the structural validity and reliability of 3D model components at an atomic level. Contemplating the antibodies own a sufficient conserved framework that accurately is predictable CDRs, and the development of algorithms used in component modeling is progressing, appropriate modeling techniques for NBs or antibodies are capable to constitute fairly proper structures (Leem et al., 2016; Weitzner et al., 2017). The NBs have VHH domains and lack VL domains but are still immensely stable. The absence of the VL domain indicates nanobodies possess a hydrophilic side as well (Siontorou, 2013).

As presented by the output of the cluster analysis in Tables 3 and 4, our data might indicate that all NBs have a reasonable affinity for the CD80/CD86. In the list of the diverse polar in-
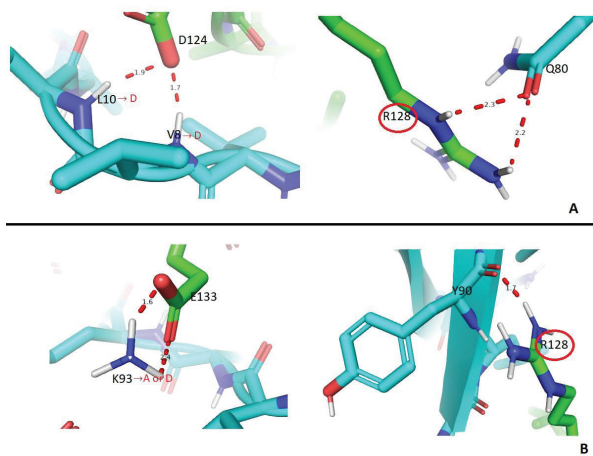
Figure 2. Cluster analysis results of reference fusion peptides by CD80. The docking complex is represented in a surface image, colored by (Abatacept and Belatacept in parts A, and B in blue color and CD80 in green). Abatacept (part A) and Belatacept (part B) commonly interact with the residue R128 on the CD80 epitope. Mutated residues of Abatacept are L10, V8→D, while Belatacept is solely K93→A or D.
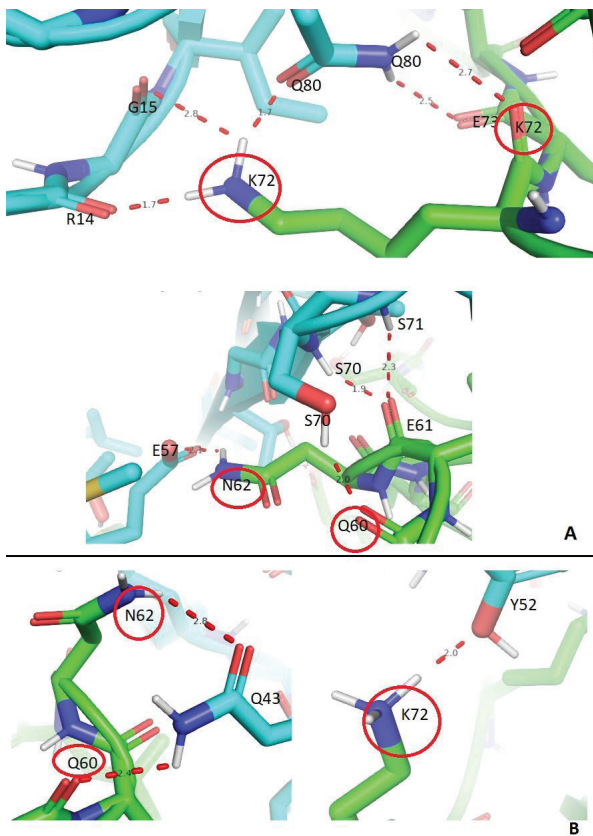
Figure 3. The Cluster analysis results of reference fusion peptides by CD86. The docking complex is depicted in a surface image, colored by (Abatacept and Belatacept in parts A, and B in blue color, and CD86 in green). Abatacept (part A) and Belatacept (part B) commonly interact with the residue Q60, N62, and K72 on the CD86 epitope.
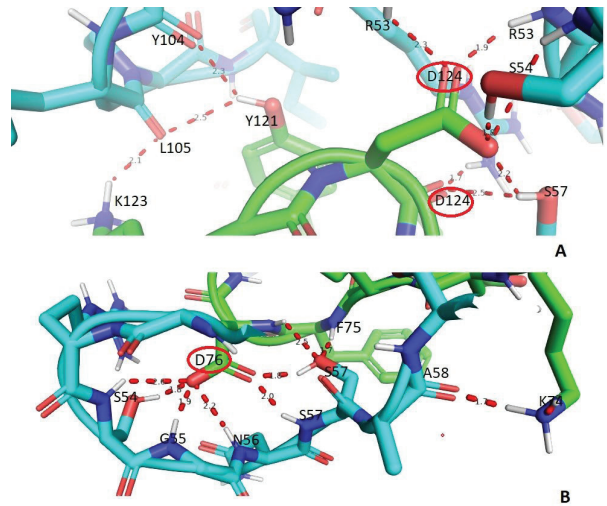
Figure 4. Part A: The most interacting region in the epitope CD80 is YEKD (121-124) and the common contact residue with model NBs is D124. Part B: In the 1A1 docking model with CD86, residue D76 in CD86 formed many polar bonds with 1A1. The docking complex is depicted in a surface image, colored by NBs in parts A, and B in blue color and CD80/86 in green).

teractions depending on the distance between the atoms of the residues, our findings showed that the CDRs of all NBs actively interact with the surface epitope residues of CD80/CD86 enacting main roles. Among six NBs, 1A1 targeting CD80 and 1B2 targeting CD86 have one of the highest performance and affinity according to the Z-scoring scale (-2.7 and -2.1). 1A1 also exhibits one of the highest avidity as it targets both CD80 and CD86 compared to Belatacept and Abatacept and the other NBs. This highest value for each CD80 and CD86 depends on both distinct the antigens epitopes on antigens and different CDRs of nbs. Most of the interacting region in the epitope CD80 is YEKD and the common contact residue is D124 from YEKD (121-124 residues) (see part A in Figure 4).

The epitope regions of CD80/86 are positioned in the Ig-like V-type domain. In the docking complexes of NBs targeting the Ig-like V-type domain, intermolecular polar bonds were formed with the residues of K120, Y121, E122, K123, D124, and R128 on the CD80-epitope, while the residues of N62,Y69, K72, K74, F75,D76 on CD86-epitope. The most common one of these binding residues of CD80 is R128 (see Figure2), while for CD86 the most common residue is D76 (see part B in Figure4). In this regard, in the 1A1 docking model, residue D76 formed many polar bonds, suggesting that it plays a significant role in affinity.

The epitope regions of CD80/86 antigens targeted in this study were also analyzed in previous studies (Mifsud et al., 2021; van Balen et al., 2020). In another study, it was shown from which residues the CD28-CD86 protein complex performs forming the interface (Krupa Pawełand Spodzieja & Sieradzan, 2021), and reported that six residues from CD86 binding to CD28 at the interaction interfaces are significant for the stability of the complex. In our results, N62, V64, E67, and Y69 of the six residues exhibited significant affinity in the interaction CD86 with nanobodies and reference peptides, and one of the most common residues at the interface of CD80-Abatacept and Be-

latacept was N62 (see Table 4 and Figure 3). In this context, the model nanobodies interacting with CD80 may effectively inhibit CD80-CD28 interaction. As mentioned previously, preventing T cell-mediated autoreactivity responses, the crucial signal of CD80/86-CD28 (Khan & Ghazanfar, 2018) seems to be an essential molecular approach for the cure of autoimmune diseases.

The molecular reason why Belatacept, a variant of the CTLA-4-Ig-like V-type domain, has higher avidity for both CD86 and CD80 than Abatacept is due to two amino acid changes (L104E and A29Y) (Larsen et al., 2005). This is in agreement with our in silico results. Only these two amino acid changes display a conformational modification in the 3D structure of Belatacept compared to Abatacept (Supplement file X) and additionally affect the docking consequence with having a higher affinity score. Nevertheless, in our docking results, no polar bond formation was observed with these altered amino acids (L104E and A29Y) to epitopes of CD80 and CD86. Our results additionally denoted, as shown with a red circle in Figure 2, that the CD80 epitope forms polar bonds with the Abatacept and Belatacept (CTLA4 variants) via the residues of V8, L10, and K93 Experimental mutagenesis studies of V8,L10, and K93, V8 → D, L10→ D and K93→A or D display that these mutations cause strongly reduced interactions with CD80 and CD86 (Ramagopal et al., 2017). Thus, possible polymorphisms and mutations in these residues may play a role in the pathogenesis of various alloreactive and autoreactive disorders.

The results, as shown with a red circle in Figures 2 and 3, indicate the residue R128 on the CD80 epitope that commonly interacts in the Abatacept and Belatacept in the complexes, just as Figure 3 exhibits the residues Q60, N62, and K72 in the Abatacept and Belatacept in the greater part of which interaction poses in the complexes. The formation of multiple polar bonds with K72 may determine its effect on the affinity and binding mode with CD86. In this context, we observed that 1B2, which has the most affinity score with CD86, also formed multiple polar bonds with K72.

Overall consequences of this study indicate that 1A1 has an affinity for CD80 and CD86 and is higher than the FDA-approved Belatacept currently in clinical use in renal transplantation. Thus it is a potential candidate for in vitro and in vivo immunosuppressant therapy investigations. In addition, the affinity of 1B2 and 2B10 to CD80 and CD86 is significantly higher than Abatacept, the first FDA-approved fusion protein in the treatment of autoimmune diseases and clinical use in rheumatoid arthritis. For this reason, 1B2 and 2B10 might be potential candidates in the treatment of autoimmune diseases.

CONCLUSION

In conclusion, to evaluate the affinity of antigen-peptide, we examined the mechanisms of interaction between nanobody models and CD80/86 and found that the interactions between them are mainly achieved by polar bonds. We found that in the CD80 epitope, most of the region interacting with NBs is the YEKD(121-124), which of the D124 residue that commonly interacts with NBs. Also, we reported that the most prevalent

interacting residue in the CD86 epitope was D76, and 1A1 has one of the highest performance and affinity according to the HADDOCK scoring scale. Additionally, we found that 1B2, the agent with the highest affinity for CD86, made multipolar bonds with the K72 residue, and we showed that the K72 residue in the CD86 epitope binds with Abatacept, and Belatacept as well. The nanobodies 1A1 and 1B2 as a result of affinity tests might be potential candidates in future immunosuppressive therapy studies. In short, our in silico approaches may contribute a source for quick and cost-effective in vitro affinity maturation of nanobody. The reader should bear in mind that the study is based on the preliminary molecular docking findings. The results of the study should be validated by molecular dynamics simulation followed by in vitro and in vivo studies.

Peer-review: Externally peer-reviewed.

Informed Consent: Written consent was obtained from the participants.

Author Contributions: Conception/Design of Study- H.İ.B., N.B., G.Y.; Data Acquisition- H.İ.B., N.B., G.Y.; Data Analysis/Interpretation- H.İ.B., N.B.; Drafting Manuscript- H.İ.B., N.B., G.Y.;Critical Revision of Manuscript- H.İ.B., N.B.; Final Approval and Accountability- H.İ.B., N.B., G.Y.

Conflict of Interest: The authors have no conflict of interest to declare.

REFERENCES

- Abbas, A. K., Lichtman, A. H., & Pillai, S. (2019). *Basic immunology e-book: Functions and disorders of the immune system*. Amsterdam, Netherlands: Elsevier Health Sciences.
- Ansari, A. W., Khan, M. A., Schmidt, R. E., & Broering, D. C. (2017). Harnessing the immunotherapeutic potential of T-lymphocyte co-signaling molecules in transplantation. *Immunology Letters*, *183*, 8–16.
- Crepeau, R. L., & Ford, M. L. (2017). Challenges and opportunities in targeting the CD28/CTLA-4 pathway in transplantation and autoimmunity. *Expert Opinion on Biological Therapy*, *17*(8), 1001–1012.
- Goronzy, J. J., & Weyand, C. M. (2008). T-cell co-stimulatory pathways in autoimmunity. *Arthritis Research & Therapy*, *10*(1), 1–10.
- Green, J. M., Noel, P. J., Sperling, A. I., Walunas, T. L., Gray, G. S., Bluestone, J. A., & Thompson, C. B. (1994). Absence of B7-dependent responses in CD28-deficient mice. *Immunity, 1*(6), 501–508.
- Janeway, C. A. J., Travers, P., Walport, M., & Shlomchik, M. J. (2001). Immunopiology: the immune system in health and disease. 5"ed. *New York*.
- Jovčevska, I., & Muyldermans, S. (2020). The therapeutic potential of nanobodies. *BioDrugs, 34*(1), 11–26.
- Khan, U., & Ghazanfar, H. (2018). T lymphocytes and autoimmunity. *International Review of Cell and Molecular Biology, 341,* 125–168.
- Krupa Pawełand Spodzieja, M., & Sieradzan, A. K. (2021). Prediction of CD28-CD86 protein complex structure using different level of resolution approach. *Journal of Molecular Graphics and Modelling, 103,* 107802.
- Larsen, C. P., Pearson, T. C., Adams, A. B., Tso, P., Shirasugi, N., Strobert, M. E., ... Peach, R. J. (2005). Rational development of LEA29Y (belatacept), a high-affinity variant of CTLA4-Ig with potent immunosuppressive properties. *American Journal of Transplantation*, *5*(3), 443-453.
- Leem, J., Dunbar, J., Georges, G., Shi, J., & Deane, C. M. (2016). A

Body Builder: Automated antibody structure prediction with data--driven accuracy estimation. *MAbs, 8*(7), 1259–1268.

• Mifsud, N. A., Illing, P. T., Lai, J. W., Fettke, H., Hensen, L., Huang, Z., ... & Purcell, A. W. (2021). Carbamazepine induces focused T cell responses in resolved Stevens-Johnson syndrome and toxic epidermal necrolysis cases but does not perturb the immunopeptidome for T cell recognition. *Frontiers in Immunology*, *12*, 653710.

• Noble, J., Jouve, T., Janbon, B., Rostaing, L., & Malvezzi, P. (2019). Belatacept in kidney transplantation and its limitations. *Expert Review of Clinical Immunology, 15*(4), 359–367.

• Pettersen, E. F., Goddard, T. D., Huang, C. C., Couch, G. S., Greenblatt, D. M., Meng, E. C., & Ferrin, T. E. (2004). UCSF Chimera—a visualization system for exploratory research and analysis. *Journal of Computational Chemistry, 25*(13), 1605–1612.

• Ramagopal, U. A., Liu, W., Garrett-Thomson, S. C., Bonanno, J. B., Yan, Q., Srinivasan, M., ... Almo, S. C. (2017). Structural basis for cancer immunotherapy by the first-in-class checkpoint inhibitor ipilimumab. *Proceedings of the National Academy of Sciences*, *114*(21), E4223-E4232.

• Raman, S., Vernon, R., Thompson, J., Tyka, M., Sadreyev, R., Pei, J. & Baker, D. (2009). Structure prediction for CASP8 with all-atom refinement using Rosetta. *Proteins: Structure, Function, and Bioinformatics*, *77*(S9), 89-99.

• Schrodinger, LLC. (2015). The {PyMOL} Molecular Graphics System, *Version*~1.8.

• Siontorou, C. G. (2013). Nanobodies as novel agents for disease diagnosis and therapy. *International Journal of Nanomedicine, 8*, 4215.

• Song, Y., DiMaio, F., Wang, R. Y.-R., Kim, D., Miles, C., Brunette, T. J., Thompson, J., & Baker, D. (2013). High-resolution comparative modeling with Rosetta CM. *Structure, 21*(10), 1735–1742.

• Sun, S., Ding, Z., Yang, X., Zhao, X., Zhao, M., Gao, L., ... Lu, X. (2021). Nanobody: a small antibody with big implications for tumor therapeutic strategy. *International Journal of Nanomedicine, 16*, 2337.

• Van Balen, P., Kester, M. G., de Klerk, W., Crivello, P., Arrieta-Bolanos, E., de Ru, A. H., ... Falkenburg, J. F. (2020). Immunopeptidome analysis of HLA-DPB1 allelic variants reveals new functional hierarchies. *The Journal of Immunology*, *204*(12), 3273-3282.

• Vita, R., Zarebski, L., Greenbaum, J. A., Emami, H., & Hoof, I. (2012). Immune Epitope Database and Analysis Resource.

• Waterhouse, A. M., Procter, J. B., Martin, D. M. A., Clamp, M., & Barton, G. J. (2009). Jalview Version 2—a multiple sequence alignment editor and analysis workbench. *Bioinformatics, 25*(9), 1189–1191.

• Waterhouse, A., Bertoni, M., Bienert, S., Studer, G., Tauriello, G., Gumienny, R., ... Schwede, T. (2018). SWISS-MODEL: homology modelling of protein structures and complexes. *Nucleic acids research*, *46*(W1), W296-W303.

• Weitzner, B. D., Jeliazkov, J. R., Lyskov, S., Marze, N., Kuroda, D., Frick, R., ... Gray, J. J. (2017). Modeling and docking of antibody structures with Rosetta. *Nature protocols*, *12*(2), 401-416.